

The various facets of liquid metal convection

Jörg Schumacher[†]

Institute of Thermodynamics and Fluid Mechanics, Technische Universität Ilmenau, D-98684 Ilmenau, Germany

Turbulent convection at low Prandtl numbers is in many aspects still *terra incognita* on the parameter map. One reason for this fact is that laboratory experiments on turbulent convection in this parameter regime are notoriously challenging as they require the use of opaque liquid metals. These working fluids prevent the application of typical optical imaging techniques such as particle image velocimetry. Recent experiments by Grannan *et al.* (*J. Fluid Mech.*, vol. 939, 2022, R1) shed new light on the variety of regimes in liquid metal flows which include rotating convection, magnetoconvection and rotating magnetoconvection next to the classical Rayleigh–Bénard case. More importantly, the authors manage the seamless crossover from one regime into another. They were thus able to study low-Prandtl-number convection at different levels of complexity in a single experimental set-up. Their work provides new insights into the tight connections between characteristic large-scale flow behaviours and the resulting global heat transfer magnitudes. This has implications for convection in planetary cores and stellar convection zones and connected dynamo action.

Key words: Bénard convection

1. Introduction

Turbulent convection flows in planetary cores and stellar interiors are the result of close interactions of buoyancy forces with magnetic fluxes, radiation, changes in chemical composition and rotation which identifies them as multi-physics processes that generate outer magnetic fields by a dynamo and release energy in stellar settings (Brandenburg & Subramanian 2005; Jones 2011; Aurnou *et al.* 2015; Schumacher & Sreenivasan 2020; Garaud 2021). In most of these cases, the molecular Prandtl number, which is defined as the ratio of the kinematic viscosity of the working fluid and its temperature diffusivity, $Pr = \nu/\kappa$, is by orders of magnitude lower than unity. In the liquid metal core of the Earth, the value is $Pr \sim 10^{-2}$; in stellar interiors $Pr \sim 10^{-6}$ or even smaller. Turbulent convection deep inside the Earth or Sun cannot be monitored directly. We have at best indirect information from magnetic fields, seismology or observations, for example of the granular cell structure at the surface of the Sun.

[†] Email address for correspondence: joerg.schumacher@tu-ilmenau.de

Laboratory experiments can therefore help us to understand some fundamental aspects of geo- and astrophysical convection in simplified set-ups under controlled conditions, despite the fact that dimensionless parameters that characterize the strength of convection will differ by many orders of magnitude. One of the most important questions is on the effectiveness of the turbulent transfer of heat and momentum depending on Prandtl and Rayleigh numbers (Kadanoff 2001). In most cases, one considers the simplest convection configuration, the Rayleigh–Bénard convection (RBC) case which applies the Boussinesq approximation (Verma 2018). The RBC system consists of a fluid layer of height H between parallel plates, uniformly heated from below and cooled from above with a temperature difference $\Delta T = T_{bottom} - T_{top} > 0$. The approximation assumes that the working fluid is incompressible, that the material parameters, such as ν and κ , are constant and that a linear dependence of the mass density field ρ on the temperature deviation from a reference equilibrium holds. The Rayleigh number which determines the thermal driving of the fluid turbulence in the layer is then defined by $Ra = g\alpha\Delta TH^3/(\nu\kappa)$, with the isobaric thermal expansion coefficient α and the acceleration due to gravity g . Experimental studies of convective turbulence in the planetary context at $Pr \sim 10^{-2}$ use opaque liquid metals, e.g. gallium, as working fluids; velocity is then accessed by ultrasound (King & Aurnou 2013; Vogt *et al.* 2018; Schindler *et al.* 2022) and cannot be obtained by optical measurements as in Aujogue *et al.* (2016).

The onset of convection is shifted to higher critical Rayleigh numbers when either the layer uniformly rotates about the vertical axis with an angular frequency Ω_0 or a magnetic field with an uniform magnetic flux density B_0 along the vertical axis penetrates the convection layer (Chandrasekhar 1961). Each extension adds a further dimensionless parameter to the convection problem. These are the Ekman number $E = \nu/(2\Omega_0 H^2)$ for the rotating case and the Chandrasekhar number $Q = \sigma B_0^2 H^2/(\rho_0 \nu)$ for the magnetoconvection (MC) case with the electrical conductivity of the fluid σ . The smaller the value of E , the stronger the rotation effects; the larger the value of Q , the stronger the magnetic field effects. The combination of rotation and magnetic fields with convection is required for a deeper understanding of the dynamos that operate in planetary and stellar interiors (Jones 2011).

2. Overview

Grannan *et al.* (2022) shed new light on exactly such a rotating MC (RMC) system in their recent experiments in liquid gallium. They set up an ever more complex convection flow step by step, starting from the well-known RBC case. Their 8.3 h experimental pub crawl displays the facets of liquid metal convection as a seamless journey from one convection case to another (see figure 1). It includes the special cases of rotating convection (RC) and MC. The experimental device consists of a closed cylindrical convection cell with an aspect ratio $\Gamma = D/H = 2$ with diameter D , filled with gallium at $Pr \simeq 0.026$. The warm-up (in its original meaning) is done with the standard RBC case at $Ra \sim 10^6$ that gives a three-dimensional large-scale circulation flow in the form of a jump rope vortex (JRV) that periodically orbits the cell (Vogt *et al.* 2018). The next stop is MC at two different Chandrasekhar numbers Q . Two magnetic field strengths have been chosen such that the ratio of magnetic forces to fluid inertia effects, which is quantified by the interaction parameter,

$$N = \frac{Q}{Re_f} = \frac{\sigma B_0^2 H}{\rho_0 U_f}, \quad (2.1)$$

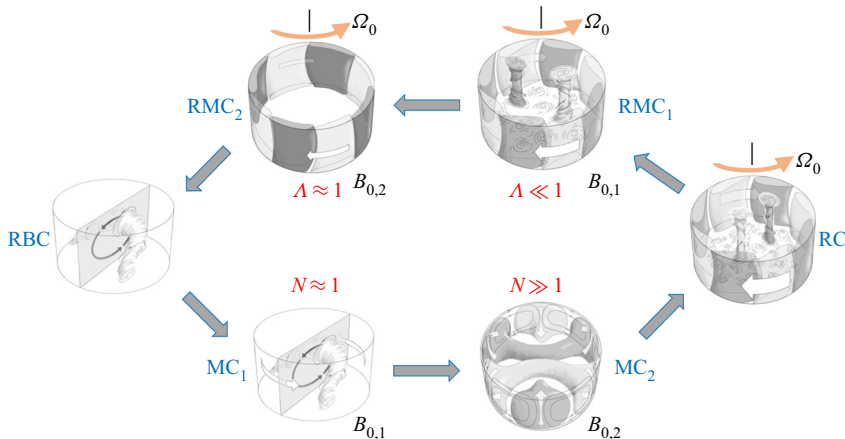


Figure 1. The experimental pub crawl starts and ends with a RBC set-up, continues with two magnetoconvection (MC) experiments at different interaction parameters N and $B_{0,1} < B_{0,2}$, stops by a rotating convection flow (RC) before passing through two rotating magnetoconvection (RMC) set-ups at different Elsässer numbers Λ .

is either unity or significantly larger. Case MC₁ with $B_{0,1}$ and $N \approx 1$ still sustains a JRV-type large-scale flow. An additional slow precession around the vertical axis is now driven by a thermoelectric net torque due to the Seebeck effect; see also Xu, Horn & Aurnou (2022). This thermoelectric effect generates additional electrical currents j_{TE} in the form of closed loops, which pass partly through each of the copper plates and the liquid metal in between, initiated by temperature gradients. These gradients are caused by impinging and ejecting large-scale plumes. As a result, thermoelectric Lorentz forces $j_{TE} \times B_0$ follow, which are different at the top and bottom of the cell thus leading to an overall net torque that moves the JRV slowly in the azimuthal direction. In case MC₂, a stronger outer magnetic field $B_{0,2} > B_{0,1}$ (and consequently $N \gg 1$) suppresses the convection flow (Chandrasekhar 1961). However, fluid motion is not fully ceased and persists in the form of wall modes – spiking, alternating upward and downward flows close to the sidewall – which cause a heat transfer that exceeds the lower diffusive bound $Nu = 1$ slightly (Zürner *et al.* 2020). They are well known from the RC flow which is the next stop of the journey (Ecke, Zhong & Knobloch 1992). The wall modes, which were fixed in position in MC₂, start to precess now due to a breaking of the azimuthal reflection symmetry in RC. This dynamics is superposed by inertial oscillations as the bulk convection is no longer suppressed. Overall, the heat transfer through the convection flow remains barely above the diffusive bound for the rest of the journey. The final two cases comprise all physical effects in RMC. The Elsässer number,

$$\Lambda = QE = \frac{\sigma B_0^2}{2\rho_0 \Omega_0}, \quad (2.2)$$

is the ratio of magnetic to Coriolis forces. For RMC₁, the magnetic field effect remains small and $\Lambda \ll 1$, such that this case does not differ significantly from its RC predecessor. The enhancement of the magnetic field back to $B_{0,2}$ drives the experiment for RMC₂ into the magnetostrophic regime with $\Lambda \approx 1$. Here, the magnetostrophic wall mode precesses at a lower drift speed than in RC or RMC₁. In the chosen parameter range, the fluid bulk should be stable which contradicts a higher measured Nu in comparison with RMC₁. Grannan *et al.* (2022) thus conclude that the slight increase of the heat transfer must be due

solely to the magnetostrophic wall mode. Their experiments highlight the importance of different macroscopic flow states for the (turbulent) heat transfer, in particular of sidewall and boundary transport. The authors have also shown that these structural changes proceed in most cases within a diffusion time $\tau_{\text{diff}} = H^2/\kappa$ without any hysteresis effects.

3. Future

What can we take home from the experimental pub crawl? (1) The thermoelectric effects, which follow when the thermal conductivity of the working fluid is not much lower than that of the bounding plate material, can lead to qualitatively new large-scale flow dynamics. Flow behaviour close to the core–mantle boundary region inside Earth (Garnero, McNamara & Shim 2016) can thus prototypically be studied in a laboratory flow and help to shed new light on the interpretation of observed planetary magnetic fields (Xu *et al.* 2022). (2) It is still open for how long the newly detected magnetostrophic wall mode will remain a dominating factor for the turbulent heat transfer once Q and Ra are increased and E is decreased and when a not-yet-discovered RMC bulk mode will start to dominate convection. Experiments at $\Gamma > 2$ will also change the role of wall modes. Even though nearly all liquid metal convection set-ups operate in the quasi-static limit where the magnetic Reynolds number $Rm \ll 1$ and magnetic field lines cannot be distorted by the turbulent flow, these experiments are thus of interest for a possible planetary dynamo. (3) Finally, the RMC experiments can provide useful information on small-scale velocity and temperature fluctuations that will lead to better estimates of eddy viscosities and diffusivities in planetary dynamo simulations. Consequently, we look forward to coming experimental pub crawls. Cheers!

Declaration of interests. The author reports no conflict of interest.

Author ORCIDs.

✉ Jörg Schumacher <https://orcid.org/0000-0002-1359-4536>.

REFERENCES

- AUJOGUE, K., POTHÉRAT, A., BATES, I., DEBRAY, F. & SREENIVASAN, B. 2016 Little Earth experiment: an instrument to model planetary cores. *Rev. Sci. Instrum.* **87** (8), 084502.
- AURNOU, J.M., CALKINS, M.A., CHENG, J.S., JULIEN, K., KING, E.M., NIEVES, D., SODERLUND, K.M. & STELLMACH, S. 2015 Rotating convective turbulence in Earth and planetary cores. *Phys. Earth Planet. Inter.* **246**, 52–71.
- BRANDENBURG, A. & SUBRAMANIAN, K. 2005 Astrophysical magnetic fields and nonlinear dynamo theory. *Phys. Rep.* **417**, 1–209.
- CHANDRASEKHAR, S. 1961 *Hydrodynamic and Hydromagnetic Stability*. Dover.
- ECKE, R.E., ZHONG, F. & KNOBLOCH, E. 1992 Hopf bifurcation with broken reflection symmetry in rotating Rayleigh–Bénard convection. *Europhys. Lett.* **19**, 177–182.
- GARAUD, P. 2021 Journey to the center of stars: the realm of low Prandtl number fluid dynamics. *Phys. Rev. Fluids* **6**, 030501.
- GARNERO, E.J., MCNAMARA, A.K. & SHIM, S.H. 2016 Continent-sized anomalous zones with low seismic velocity at the base of Earth's mantle. *Nat. Geosci.* **9**, 481–489.
- GRANNAN, A.M., CHENG, J.S., AGGARWAL, A., HAWKINS, E.K., XU, Y., HORN, S., SÁNCHEZ-ÁLVAREZ, J. & AURNOU, J.M. 2022 Experimental pub crawl from Rayleigh–Bénard to magnetostrophic convection. *J. Fluid Mech.* **939**, R1.
- JONES, C.A. 2011 Planetary magnetic fields and fluid dynamos. *Annu. Rev. Fluid Mech.* **43**, 583–614.
- KADANOFF, L.P. 2001 Turbulent heat flow: structures and scaling. *Phys. Today* **54**, 34–39.
- KING, E.M. & AURNOU, J.M. 2013 Turbulent convection in liquid metal with and without rotation. *Proc. Natl Acad. Sci. USA* **110**, 6688–6693.
- SCHINDLER, F., ECKERT, S., ZÜRNTER, T., SCHUMACHER, J. & VOGT, T. 2022 Collapse of coherent large scale flow in strongly turbulent liquid metal convection. *Phys. Rev. Lett.* **128**, 164501.

The various facets of liquid metal convection

- SCHUMACHER, J. & SREENIVASAN, K.R. 2020 Colloquium: unusual dynamics of convection in the Sun. *Rev. Mod. Phys.* **92**, 041001.
- VERMA, M.K. 2018 *Physics of Buoyant Flows*. World Scientific.
- VOGT, T., HORN, S., GRANNAN, A.M. & AURNOU, J.M. 2018 Jump rope vortex in liquid metal convection. *Proc. Natl Acad. Sci. USA* **115**, 12674–12679.
- XU, Y., HORN, S. & AURNOU, J.M. 2022 Thermoelectric precession in turbulent magnetoconvection. *J. Fluid Mech.* **930**, A8.
- ZÜRNER, T., SCHINDLER, F., VOGT, T., ECKERT, S. & SCHUMACHER, J. 2020 Flow regimes of Rayleigh–Bénard convection in a vertical magnetic field. *J. Fluid Mech.* **894**, A21.